ChemPubSoc Europe

DOI: 10.1002/batt.201900051

BATTERIES & SUPERCAPS Communications

Stable Acetals of Glyoxal as Electrolyte Solvents for Lithium-Ion Batteries

Lars H. Hess,[a, b] Simon Wankmüller,[a, b] Lukas Köps,[a, b] Annika Bothe,[a, b] and Andrea Balducci*[a, b]

In this manuscript, we report for the first time about the use of the glyoxylic-acetals-based electrolytes in combination with graphite electrodes. We showed that these innovative electrolytes display good viscosities and conductivities, as well as higher thermal stability and flash points compared to the electrolyte based on conventional solvents. Additionally, they display intrinsic film-forming ability and they can be successfully used in combination with graphite electrodes.

The realization of lithium-ion batteries (LIBs) with improved safety with respect to the state-of-the-art devices represents one of the most critical challenges for the future of this key technology.[1] As reported in many studies, the flammability, toxicity and the limited temperature range of use of the organic electrolyte mixtures used nowadays in commercial devices are seriously limiting the safety of LIBs.[1a,2] In the last years several alternative electrolyte components have been considered, and a large number of alternative organic solvents and salts have been proposed.[3] Furthermore, great efforts have been dedicated to the investigation of ionic-liquid-based electrolytes.[4] So far, although interesting results have been obtained none of the proposed alternatives have been massively introduced into commercial devices.

The electrolyte of LIBs needs to display low toxicity, low flammability and good environmental degradability.[5] Furthermore, it should display high chemical and electrochemical stability and, at the same time, the ability to form effective passive layer(s), e.g. to form a good solid electrolyte interface (SEI). Finally, it should be easy to synthesize (in large volume) and to be cost efficient.[6] Clearly, it is extremely difficult to find a chemical compound able to display all these properties simultaneously. For these reasons, the use of multicomponent electrolyte systems, e.g., containing more than one solvent, has been the strategy of choice so far.[1b] The use of these multicomponent systems is certainly advantageous for the design of electrolytes able to fulfill most of the abovementioned properties. Nevertheless, it is important to remark that this approach is not free of limitations. For example, linear carbonates, e.g., dimethyl carbonate (DMC), are largely used in LIBs due to their low viscosity, which is beneficial for the battery performance. However, these linear carbonates are typically flammable, while displaying a low boiling point and thus their use is limiting the safety of LIBs.[1a] Additionally, they typically do not display SEI forming ability.[7] The introduction of alternative solvents with improved properties in comparison to linear carbonates would be therefore beneficial for the realization of safer LIBs.[1d]

In a recent work, we proposed the use of the solvents tetraethoxy glyoxal (TEG) and tetramethoxy glyoxal (TMG), which are belonging to the chemical family of carbonyl derivatives, as electrolyte components for energy storage devices.[8] Acetals such as TEG and TMG have not a very high dielectric constant but they usually display low viscosity and very low melting points.[9] TEG and TMG are commercially available, and their price is comparable to that of other solvents currently used in energy storage devices.[8] Both of them can be used to dissolve a large number of salts and, very importantly, they display very low toxicity.[8]

In our previous investigation we used these solvents in combination with activated carbon-based electrodes and with lithium iron phosphate-based electrodes. In this work we report for the first time the use of TMG- and TEG-based electrolytes in combination with graphite electrodes, which are the state-of-the-art anodes of LIBs. This study is of importance to understand the effective applicability of these solvents in LIBs.

The electrolytes 1 M LiTFSI in TEG and 1 M LiTFSI in TMG display similar conductivities and viscosities in a broad range of temperature.[8] At 20 °C both electrolytes display a conductivity of 1.5 mS cm^{-1}, while at 80 °C the conductivity of the electrolyte containing TMG (5.4 mS cm^{-1}) is higher than that containing TEG (4.6 mS cm^{-1}) (more details are reported in Figure S1). Although these conductivities values are not superior to those displayed by conventional electrolytes, they are comparable to those of other alternative electrolytes, e.g. ionic liquids (ILs), and they appear sufficiently high for application in LIBs.[1b,10] At 20 °C the electrolyte 1 M LiTFSI in TEG displays a viscosity of 8.8 mPa s, while the viscosity of 1 M LiTFSI in TMG is equal to 11 mPa s. These values of viscosities are comparable to those reported for many alternative electrolytes for LIB.[3a,4e,g,11] Electrolyte density is an important parameter for the validation

[a] L. H. Hess, S. Wankmüller, L. Köps, A. Bothe, Prof. Dr. A. Balducci
Institute for Technical Chemistry and Environmental Chemistry, Friedrich Schiller University Jena,
Philosophenweg 7a, 07743 Jena, Germany
E-mail: andrea.balducci@uni-jena.de

[b] L. H. Hess, S. Wankmüller, L. Köps, A. Bothe, Prof. Dr. A. Balducci
Center for Energy and Environmental Chemistry Jena (CEEC Jena), Friedrich Schiller University Jena,
Philosophenweg 7a, 07743 Jena, Germany

Supporting information for this article is available on the WWW under https://doi.org/10.1002/batt.201900051

of theoretical investigations and important for the cost evaluation of the electrolyte. Figure S1 compares the densities of the electrolytes between 10 °C and 80 °C. Although the variation of density is following a similar behavior for both electrolytes, it is interesting to notice that the electrolyte containing TMG is nearly 0.1 g ml^{-1} denser than that containing TEG. At 20 °C the densities of 1 M LiTFSI in TEG and 1 M LiTFSI in TMG are equal to 1.08 g ml^{-1} and 1.17 g ml^{-1}, respectively. Figure 1 is comparing the electrochemical stability of the

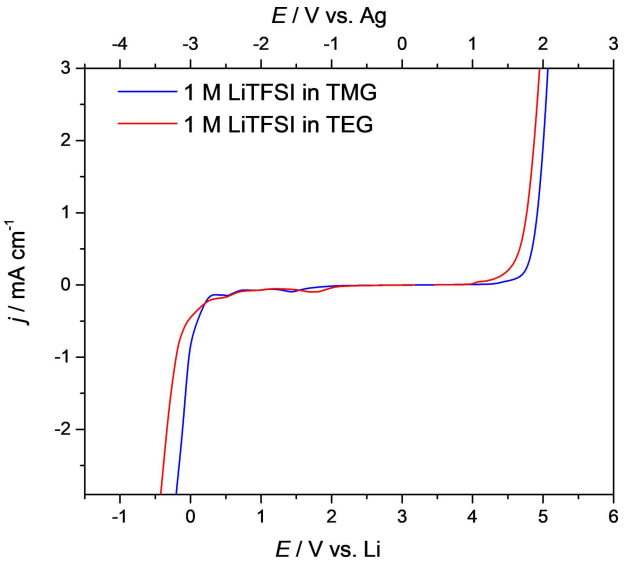

Figure 1. Electrochemical stability at room temperature (scan rate: 1 mV s^{-1}) of the electrolytes consisting of 1 M LiTFSI in TMG and 1 M LiTFSI in TEG.

electrolytes 1 M LiTFSI in TEG and 1 M LiTFSI in TMG at 20 °C against a platinum working electrode. As shown in the figure, the electrolytes display a good cathodic stability, and both of them are stable until the potential of the Li plating (0 V vs. Li/Li$^+$). Nevertheless, from the figure it can be noticed that the electrolyte containing TEG appears slightly more stable than the one containing TMG, which is showing some minor peaks in the region between 1.5 and 0.5 V vs. Li/Li$^+$. As shown in the figure, the anodic stability of the electrolytes is ca. 4.5 V vs. Li/Li$^+$. The overall ESW of both electrolytes is therefore in the order of 4.5 V, which is a value large enough for the use in LIBs.

The thermal stability of the electrolyte is affecting the temperature range of use and by this the safety of LIBs, it is therefore a key parameter for these devices. Figure 2a is comparing the thermal stability of neat TEG with neat TMG. To have a more straightforward comparison with the state-of-the art electrolyte of LIBs, also DMC is included on the figure. As shown, TEG is stable up to ca. 80 °C (5% weight loss), while TMG starts losing weight already at 50 °C. Both glyoxylic acetals are significantly more stable than DMC, which is evaporating already slightly above room temperature. These differences are maintained when a lithium salt, in this case LiTFSI, is added to the solvent to realize an electrolytic solution suitable for use in LIBs. As shown in Figure 2b, all three electrolytes display a big weight loss from room temperature until 100 °C, which is

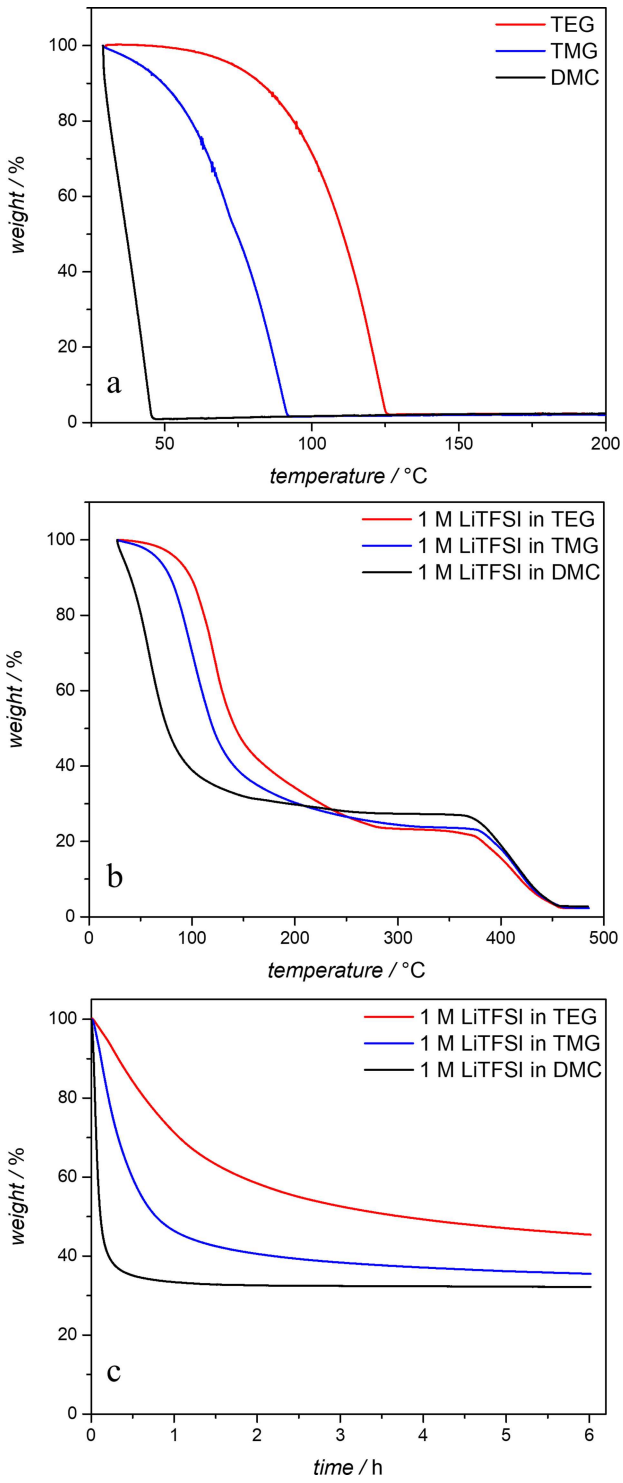

Figure 2. Thermogravimetric analysis: temperature ramp at 10 °C min^{-1} of neat solvent (a) and investigated electrolytes (b); isothermal at 60 °C for 6 hours of the investigated electrolytes (c).

associated to the solvent evaporation. However, the temperature at which this loss begins is strongly depending on the nature of the solvent, and the use of TEG and TMG allows a much higher stability compared to the use of DMC. Above 400 °C, the lithium salt decomposes, causing the second significant weight loss. Since the nature and the molarity of the

salt are the same in all electrolytic solutions, the behavior at high temperature of the electrolytes is very comparable in this region. To further investigate the thermal properties of the electrolytes also isothermal TGA experiments have been carried out. In this case, the electrolytes were kept at 60 °C for 6 hours. As shown in Figure 2c, after this time the electrolyte containing DMC was able to retain 35% of its initial weight. This weight, which corresponds to the weight of the salt in the electrolyte, is indicating that at the end of the experiment all DMC evaporated from the electrolyte. The weight retention of the glyoxal-based electrolytes was higher, showing that in these solutions the solvent was not evaporating as fast as the conventional DMC. Among the three solvents, TEG appears to be the least volatile, as indicated by the fact that after 6 hours 1 M LiTFSI in TEG was able to retain 50% of its initial weight. These results are clearly indicating that TEG and TMG display an improved thermal stability compared to DMC. Additionally, it is also important to mention that these two solvents display a much higher flash point than DMC: 72 °C, 52 °C, 16 °C[12] for TEG, TMG and DMC, respectively. Taking these results into account TEG and TMG appear to display an interesting set of properties for the use in LIBs.

As mentioned in the introduction, glyoxal-based electrolytes have never been tested in combination with graphite electrodes. Since these electrodes are the state-of-the-art anode in LIBs, this investigation appears of great importance to evaluate the use of these novel electrolytes in these devices. Figure 3 is illustrating the behavior of graphite electrodes in combination with 1 M LiTFSI in TEG and 1 M LiTFSI in TMG. As shown, the use of both electrolytes enables a reversible insertion-extraction of lithium-ions into graphite. This is well observable in the CV profiles (Figure 3a) as well as on charge-discharge curves (Figure 3b). As shown in the inset of Figure 3b, the variation of the differential capacity[13] of the electrodes over the potential is displaying the typical stage of intercalation (and extraction) of lithium into graphite. Considering these results, both electrolytes appear to have intrinsic film forming ability. Among them, 1 M LiTFSI in TEG is the one allowing the higher reversibility and the higher coulombic efficiency during the charge-discharge process (96% and 98% in 1 M LiTFSI in TMG and 1 M LiTFSI in TEG, respectively, after 5 cycles).

As indicated in Figure 3c, at 0.1 C the graphite electrode cycled in 1 M LiTFSI in TMG delivers a discharge capacity of 330 mAh g^{-1}, while the capacity delivered by the electrode cycled in 1 M LiTFSI in TEG was 340 mAh g^{-1}. At 1 C the electrode discharge capacity decreased and was equal to 140 mAh g^{-1} and 160 mAh g^{-1} in 1 M LiTFSI in TMG and 1 M LiTFSI in TEG, respectively. Taking into account the viscosity/conductivity of the investigated electrolytes and the fact that no SEI additives were used, these values of capacity are certainly very promising. It is also important to notice that these values are higher than those of other alternative electrolytes proposed in the past, e.g., based on ionic liquids, cycled in comparable conditions.[14] As shown in Figure 3c, the electrode cycled in 1 M LiTFSI in TMG displays a lower stability over the charge-discharge process compared to that cycled in 1 M LiTFSI in TEG. As visible on the figures, after the test carried out at different C-rates the graphite electrode cycled in this latter electrolyte was able to recover almost all its initial capacity.

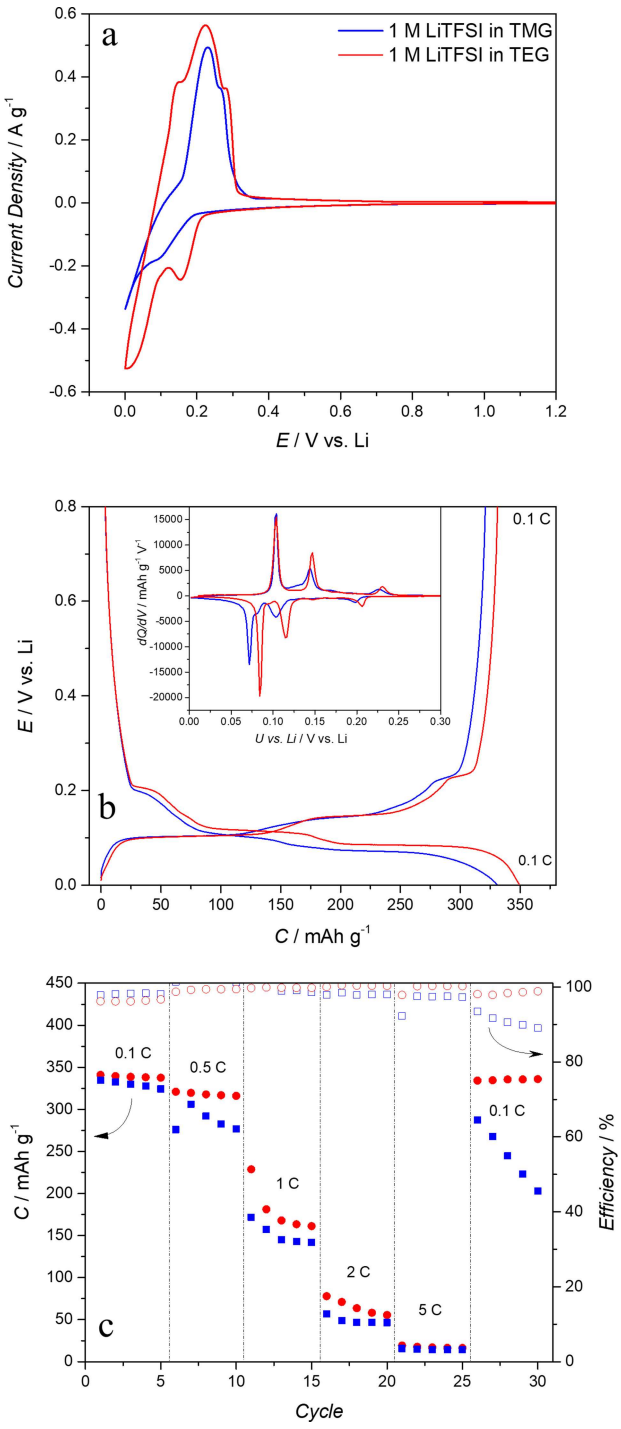

Figure 3. Graphite electrodes in combination with the electrolytes 1 M LiTFSI in TMG and 1 M LiTFSI in TEG: (a) Cyclic voltammetry at 0.1 mV s^{-1}; (b) comparison of charge-discharge voltage profile and differential capacity (inset) at 0.1 C and (c) capacity retention during charge-discharge carried out at different C-rates.

With the aim to understand the impact of the addition of a film additive on the behavior of graphite electrodes cycled in glyoxal-based electrolytes, also tests with the electrolytes

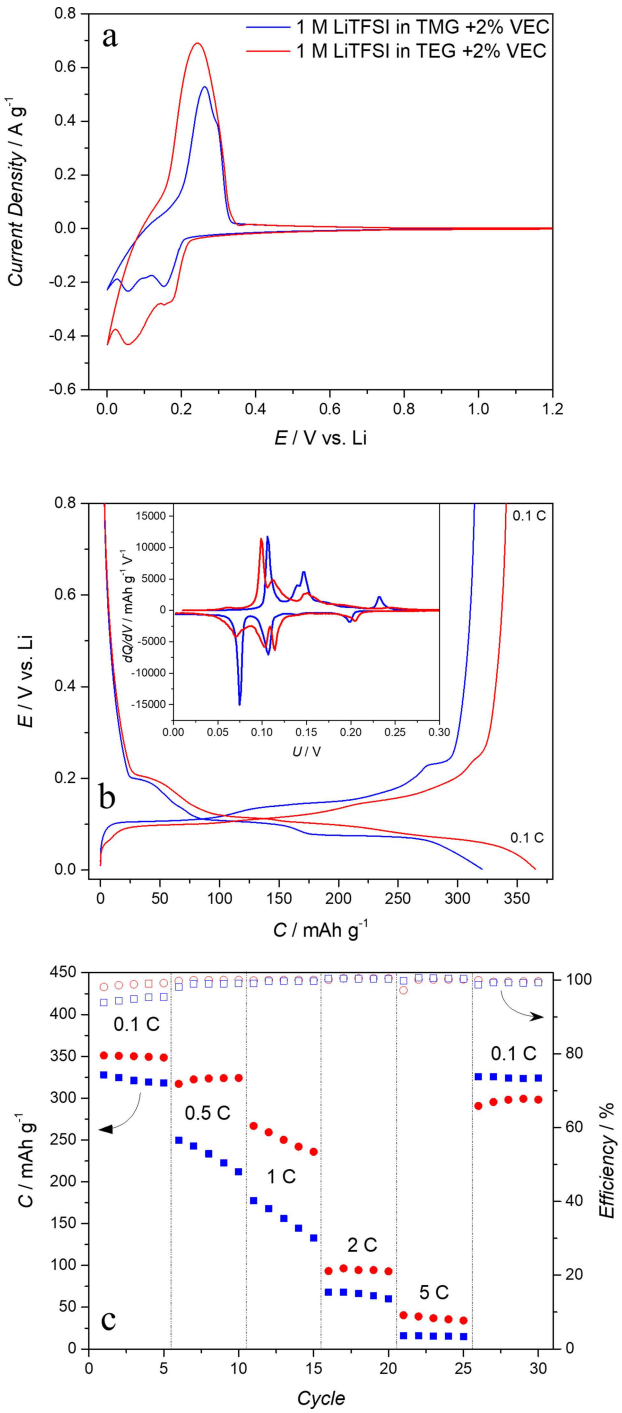

Figure 4. Graphite electrodes in combination with the electrolytes 1 1 M LiTFSi in TMG + 2% VEC and 1 M LiTFSI in TEG + 2% VEC: (a) Cyclic voltammetry at 0.1 mV s^{-1}; (b) comparison of charge-discharge voltage profile and differential capacity (inset) at 0.1 C and (c) capacity retention during charge-discharge carried out at different C-rates.

containing 2% vinyl ethylene carbonate (VEC) have been considered. The results of these tests are reported in Figure 4. As shown in Fig. 4a the addition of VEC to the electrolytes is modifying the CV profiles of the electrodes, making better visible the reduction and oxidation peaks associated to the stages of insertion and extraction within the layered structure of graphite. This improved reversibility is also visible on the charge-discharge curves as well as on the variation of the differential capacity of the graphite electrodes over the potential (Figure 4b). Furthermore, also the efficiency of the charge-discharge process was improved by the addition of VEC (98% and 99% in 1 M LiTFSI in TMG + 2%VEC and 1 M LiTFSI in TEG + 2%VEC, respectively, after 4 cycles). At 0.1 C the graphite electrode cycled in 1 M LiTFSI in TMG + 2%VEC delivers a discharge capacity of 320 mAh g^{-1}. In the case of TEG, the addition of the additive is improving the discharge capacity delivered by the electrode to 350 mAh g^{-1}, which is a value close to the theoretical capacity of graphite. At 1 C, the electrode capacity decreased, as expected, but the entity of this decrease was significantly affected by the nature of the electrolyte. While the electrode cycled in 1 M LiTFSI in TMG + 2%VEC delivered a capacity of ca. 125 mAh g^{-1}, the one cycled in 1 M LiTFSI in TEG + 2%VEC was able to deliver a capacity of 240 mAh g^{-1}. As shown in the figure, after the test carried out at different C-rates the graphite electrodes cycled in both electrolytes were able to recover a large fraction of their initial capacity and were able to display a stable behavior. Taking these results into account, the addition of additive appears therefore to improve the efficiency of the charge-discharge process as well as the electrode capacity, especially in the case of TEG-based electrolytes.

After cycling, the graphite electrodes cycled in the glyoxal solvents have been investigated by ex-situ SEM and EDX analysis. Figure 5 shows the overlay of the EDX analysis with the SEM image. The pristine graphite sample has been marked with a turquoise colour. As shown, all cycled electrodes show residues generated by the decomposition of the electrolyte (the red rods visible on the SEM are fragments of the employed glass fibre separator). In all electrodes the presence of fluorine and sulfur compounds (marked by yellow and purple pixels, respectively) is visible on the electrode surface, indicating the formation of a (passive) layer originated by the decomposition of both, $TFSI^-$ anion and solvent molecules. Furthermore, for all electrolytes (b-e), the sharp edges of the pristine graphite are superimposed by what clearly are covering layers of decomposition products. Taking these results into account, the high efficiency and good cycling stability of the investigated electrodes, it is reasonable to assume that glyoxal-based electrolytes are able to form a stable SEI on the graphite electrodes.

In conclusion, the results of this investigation showed, for the first time, that glyoxylic-acetal-based electrolytes can be successfully used in combination with graphite electrodes, and that the solvents TEG and TMG have intrinsic film-forming ability. The addition of a film-forming additive is improving the electrode performance and, very interestingly, we showed that electrodes cycled in 1 M LiTFSI in TEG + 2%VEC are able to deliver a capacity of 350 mAh g^{-1} at room temperature. Taking these results into account, and the fact that TEG and TMG display a good set of transport and thermal properties and a higher flash point compared to DMC, the investigated solvents appear very promising in view of the realization of advanced and safer LIBs. Work is now in progress to investigate the use of these electrolytes in full LIB cells, to investigate the proper-

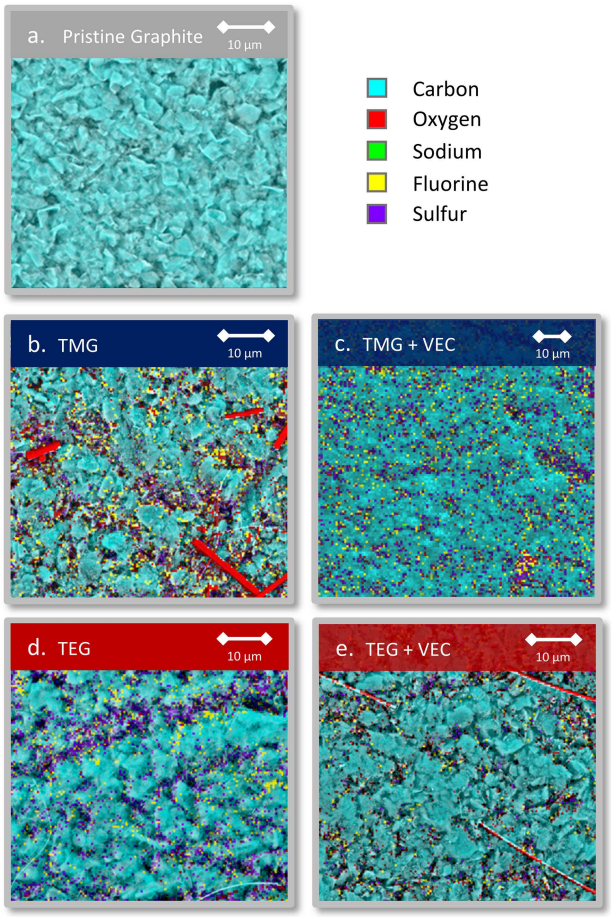

Figure 5. Overlay of SEM and EDX measurements of at the pristine graphite electrodes and b-e the ex-situ graphite electrodes after cycling. 4b shows the graphite electrode in the TMG-based electrolyte, while 4c shows the combination of TMG and VEC. 4d shows the TEG-based electrolyte, while 4e shows the TEG-based electrolyte in combination with VEC.

ties of electrolytes based on mixtures containing glyoxylic acetals and conventional solvents, e.g. EC and DMC, and to investigate in depth the composition of the SEI in these solvents. This investigation will make possible a better comparison of these novel electrolytes with the state-of-the art and, thus, a more precise assessment about the advantages related to their use in LIBs.

Experimental Section

The solvents tetramethoxyglyoxal (TMG) and tetraethoxyglyoxal (TEG) have been supplied by Weylchem. After drying as described in reference,[8] both solvents displayed a water content equal to 20 ppm, as measured by Karl-Fischer titration. The solvents were used in combination with lithium bis(trifluoromethanesulfonyl) imide (LiTFSI) purchase by Solvionic. The additive Vinyl Ethylene Carbonate (VEC) was purchased by Sigma Aldrich. All electrolytes investigated in this study displayed a water content lower than 20 ppm, as measured by Karl-Fischer titration. The conductivity of the investigated electrolytes has been measured using a ModuLab XM ECS Potentiostat in the temperature range comprise between −20 °C and 80 °C following a procedure identical to that reported in reference.[15] The viscosity of the electrolytes has been determined by using an "Anton Paar" MCR 102 rotational viscometer at 20 °C with a shear rate of 2000 1/s.[15] The density was determined by using an oscillating U-tube densitometer DMA 4100 M from "Anton Paar" in a temperature range between 10 °C and 80 °C.The thermal analysis was performed with a Perkin Elmer STA 6000 using nitrogen as carrier gas with a total flow rate of 60 ml/min. The heating rate for ramp experiments was 10 °C/min. All the electrochemical tests have been carried out utilizing Swagelok type cells, which were assembled in an argon-filled glove box (H_2O and $O_2 < 1$ ppm). For the determination of the electrochemical stability window (ESW) a three-electrode set-up was applied using a Pt-microelectrode as working electrode (WE), an oversized activated carbon (AC) electrode as counter electrode (CE) and a silver wire as reference electrode (RE). Graphite composite electrodes were prepared according to Ref. [30]. The graphite electrodes contained 90 wt% graphite (Imerys, Switzerland), 5 wt% Super C65 (Imerys, Switzerland) and 5 wt% sodium carboxymethylcellulose (CMC, Walocel CRT 2000 PA, Dow Wolff Cellulosics, Germany) as binder. The electrode area was 1.13 cm^2 and the active mass loading of graphite electrodes was between 0.5 mg and 1.5 mg per electrode. In the electrochemical tests the graphite-based electrode was used as working electrode, while metallic lithium was used as counter electrode and also as reference electrode. In all tests, glass fibre Whatman separators (520 µm) were used as separator, which have been filled with 120 µL of electrolyte. Flash Points, if not stated else, were determined by a Normalab NPV 310 with gas ignition using 2 ml of solvent in the rapid equilibrium closed cup method according to ISO 3679. SEM and EDX analysis have been conducted on a Phenom ProX Desktop SEM at 10 kV and 15 kV utilizing charge reduction mode in order to reduce artifacts by electrostatic charging of the sample.

Acknowledgements

The authors wish to thank the Deutsche Forschungsgemeinschaft (DFG) within the project "The combined use of computational screening and electrochemical characterization for the identification of new electrolyte components for supercapacitors" for the financial support. Furthermore, they wish to thank the company Weylchem for kindly supplying TEG and TMG.

Conflict of Interest

The authors declare no conflict of interest.

Keywords: lithium-ion batteries · glyoxal · acetal · electrolyte · graphite

[1] a) D. H. Doughty, E. P. Roth, *Interface magazine* **2012**, *21*, 37–44; b) J. Kalhoff, G. G. Eshetu, D. Bresser, S. Passerini, *ChemSusChem* **2015**, *8*, 2154–2175; c) S. Abada, G. Marlair, A. Lecocq, M. Petit, V. Sauvant-Moynot, F. Huet, *J. Power Sources* **2016**, *306*, 178–192; d) P. G. Balakrishnan, R. Ramesh, T. Prem Kumar, *J. Power Sources* **2006**, *155*, 401–414.
[2] a) G. Zubi, R. Dufo-López, M. Carvalho, G. Pasaoglu, *Renew. Sust. Energy Rev.* **2018**, *89*, 292–308; b) Q. Wang, P. Ping, X. Zhao, G. Chu, J. Sun, C. Chen, *J. Power Sources* **2012**, *208*, 210–224.
[3] a) S. Brox, S. Röser, T. Husch, S. Hildebrand, O. Fromm, M. Korth, M. Winter, I. Cekic-Laskovic, *ChemSusChem* **2016**, *9*, 1704–1711; b) S.

Nowak, M. Winter, *J. Electrochem. Soc.* **2015**, *162*, A2500–A2508; c) M. Dahbi, F. Ghamouss, F. Tran-Van, D. Lemordant, M. Anouti, *J. Power Sources* **2011**, *196*, 9743–9750; d) L. Hu, S. S. Zhang, Z. Zhang, in *Rechargeable Batteries: Materials, Technologies and New Trends* (Eds.: Z. Zhang, S. S. Zhang), Springer International Publishing, Cham, **2015**, pp. 231–261; e) A. Lex-Balducci, P. Isken, R. Schmitz, C. Dippel, M. Kunze, M. Winter, in *Meeting Abstracts*, The Electrochemical Society, **2010**, pp. 591–591; f) T. Husch, N. D. Yilmazer, A. Balducci, M. Korth, *Phys. Chem. Chem. Phys.* **2015**, *17*, 3394–3401; g) M. Korth, *Phys. Chem. Chem. Phys.* **2014**, *16*, 7919–7926.

[4] a) D. R. MacFarlane, N. Tachikawa, M. Forsyth, J. M. Pringle, P. C. Howlett, G. D. Elliott, J. H. Davis, M. Watanabe, P. Simon, C. A. Angell, *Energy Environ. Sci.* **2014**, *7*, 232–250; b) A. Guerfi, M. Dontigny, P. Charest, M. Petitclerc, M. Lagacé, A. Vijh, K. Zaghib, *J. Power Sources* **2010**, *195*, 845–852; c) K. Ueno, R. Tatara, S. Tsuzuki, S. Saito, H. Doi, K. Yoshida, T. Mandai, M. Matsugami, Y. Umebayashi, K. Dokko, *Phys. Chem. Chem. Phys.* **2015**, *17*, 8248–8257; d) M. Nádherná, J. Reiter, J. Moškon, R. Dominko, *J. Power Sources* **2011**, *196*, 7700–7706; e) R. S. Kühnel, N. Böckenfeld, S. Passerini, M. Winter, A. Balducci, *Electrochim. Acta* **2011**, *56*, 4092–4099; f) S. Menne, J. Pires, M. Anouti, A. Balducci, *Electrochem. Commun.* **2013**, *31*, 39–41; g) J. R. Nair, F. Colò, A. Kazzazi, M. Moreno, D. Bresser, R. Lin, F. Bella, G. Meligrana, S. Fantini, E. Simonetti, G. B. Appetecchi, S. Passerini, C. Gerbaldi, *J. Power Sources* **2019**, *412*, 398–407; h) A. Basile, A. I. Bhatt, A. P. O'Mullane, *Nat. Commun.* **2016**, *7*, ncomms11794.

[5] A. M. Bernardes, D. C. R. Espinosa, J. A. S. Tenório, *J. Power Sources* **2004**, *130*, 291–298.

[6] a) D. Larcher, J. M. Tarascon, *Nat. Chem.* **2015**, *7*, 19–29; b) D. L. Wood, J. Li, C. Daniel, *J. Power Sources* **2015**, *275*, 234–242.

[7] M. C. Smart, *J. Electrochem. Soc.* **1999**, *146*, 486.

[8] L. H. Hess, A. Balducci, *ChemSusChem* **2018**, *11*, 1919–1926.

[9] B. Flamme, G. Rodriguez Garcia, M. Weil, M. Haddad, P. Phansavath, V. Ratovelomanana-Vidal, A. Chagnes, *Green Chem.* **2017**, *19*, 1828–1849.

[10] J. Alvarado, M. A. Schroeder, M. Zhang, O. Borodin, E. Gobrogge, M. Olguin, M. S. Ding, M. Gobet, S. Greenbaum, Y. S. Meng, K. Xu, *Mater. Today* **2018**, *21*, 341–353.

[11] a) C.-C. Su, M. He, P. C. Redfern, L. A. Curtiss, I. A. Shkrob, Z. Zhang, *Energy Environ. Sci.* **2017**, *10*, 900–904; b) E. Kovalska, C. Kocabas, *Mater. Today Commun.* **2016**, *7*, 155–160; c) Y.-S. Ye, J. Rick, B.-J. Hwang, *J. Mater. Chem. A* **2013**, *1*, 2719–2743.

[12] S. Hess, M. Wohlfahrt-Mehrens, M. Wachtler, *J. Electrochem. Soc.* **2015**, *162*, A3084–A3097.

[13] a) A. Smith, J. Dahn, *J. Electrochem. Soc.* **2012**, *159*, A290–A293; b) A. Smith, J. Burns, J. Dahn, *Electrochem. Solid-State Lett.* **2011**, *14*, A39-A41.

[14] A. Balducci, *Top. Curr. Chem.* **2017**, *375*, 20.

[15] L. H. Hess, A. Balducci, *Electrochim. Acta* **2018**, *281*, 437–444.

Manuscript received: April 8, 2019
Revised manuscript received: July 24, 2019
Accepted manuscript online: July 26, 2019
Version of record online: August 8, 2019